Cluster Characteristics of Wideband 3D MIMO Channels in Outdoor-to-Indoor Scenario at 3.5 GHz

Detao Du, Jianhua Zhang, Chun Pan, Chi Zhang
Key Laboratory of Universal Wireless Communications,
Wireless Technology Innovation Institute, Ministry of Education,China
Beijing University of Posts and Telecommunications, Beijing, 100876, China
Email: detaodu@gmail.com

***Abstract*—In this paper, we present a cluster parameter based analysis of an outdoor-to-indoor (O2I) Multiple-Input-Multiple-Output (MIMO) measurement campaign carried out at 3.5 GHz in an office building. The measurement was performed using a wideband multi-antenna radio channel sounder. Besides azimuth angle of arrival (AoA), azimuth angle of departure (AoD) and delay domains included in traditional 2 dimensional (2D) MIMO channels, 3 dimensional (3D) MIMO channels also consider elevation angle of arrival (EoA), elevation angle of departure (EoD) when describing clusters. By introducing the elevation domain, we observe that multipath components (MPCs) within one cluster in 2D MIMO channels can be divided into several clusters in 3D MIMO channels and each cluster has MPCs with smaller power weighed multipath component distance (MCD). We also analyze the effect of height difference between the transmitting and receiving ends on the clustering performance. There is a tendency that clusters show smaller parameter values when the height difference is smaller. After that, we describe all the cluster parameters by a set of probability density functions (pdfs) and give typical values in this scenario.**

I. Introduction

The use of multiple antennas at both link ends in wireless communication systems can promise tremendous capacity improvements compared to single antenna systems. Ultimately, the capacity gains depend on the channel model in which the system is operating. Thus, Multiple-Input-Multiple-Output (MIMO) channel modeling becomes necessary.

An important feature of the MIMO propagation channels is the occurrence of multipath components (MPCs) within clusters showing similar parameters such as azimuth angle of arrival (AoA), azimuth angle of departure (AoD), elevation angle of arrival (EoA), elevation angle of departure (EoD), and delay [1-2]. Having a knowledge of the characteristics of clusters means a better understanding of the propagation mechanism of the channel. What's more, sometimes a global angular spread (AS) is not able to capture the detailed structure of the direction in the radio propagation channels which is crucial for a number of MIMO transmission techniques, e.g. [3]. In addition, clustering can have a significant impact on channel capacity. Many advanced radio channel models are based on the concept of multipath clusters. And according to [4], unclustered models tend to overestimate the capacity if the MPCs are indeed clustered. Furthermore, from an aspect of system level evaluation, it is convenient to model the propagation channel in terms of cluster properties rather than model the behavior of individual MPCs.

There have been studies about cluster-level parameters in different scenarios [5-8]. Most of them concerned only about AoA-AoD-delay domains. Recently, 3 dimensional (3D) MIMO has been identified as one important technique for performance enhancement in LTE Release 12 for 3rd Generation Partnership Project (3GPP) [9] and M.Shafi has extended the spatial channel model (SCM) to 3D [10]. World Wireless Initiative New Radio + (WINNER+) report summarizes some results at the mobile station (MS) in terms of the AS and attempts to extend the 2 dimensional (2D) geometry based stochastic model (GBSM) into 3D [11]. From January 2013, 3GPP Technical Specification Group-Radio Access Network (TSG-RAN) Working Group 1 (WG1) also initiates the discussion on the 3D fading channel model. Since 3D MIMO is so important, it is necessary for us to take the elevation domain into consideration when clustering the MPCs.

In this paper, we adopt the automatic clustering algorithm proposed in [12], which used multipath component distance (MCD) as the distance function [13] and included path power into the cluster identification. Clusters are identified jointly on the AoA, AoD, EoA, EoD and delay domains. To the author's knowledge this is the first paper to present a full framework for cluster identification in outdoor-to-indoor (O2I) scenario in 3D MIMO channels. Traditional channel models, such as the International Telecom Union-Radio communication Sector (ITU-R) M.2135 channel model, only concerned about 2D channels. Furthermore, due to height difference between the transmitting and receiving ends, differences of the statistical properties of the clusters are analyzed.

The rest of the paper is organised as follows. Section II describes the measurement equipment and environment. In section III, data processing is introduced. Clustering results based on the measurement data are presented in section IV. Finally, section V concludes the paper.

II. Measurement Description

A. Measurement System

The measurement was performed on the campus of Beijing University of Posts and Telecommunications (BUPT), China, utilizing the Elektrobit Propsound Sounder at a carrier frequency of 3.5 GHz and a signal bandwidth of 100 MHz. As shown in Fig. 1, the transmitting side (Tx) employs a uniform

(a) UPA (b) ODA

Fig. 1. Antenna arrays used in channel measurements

patch array (UPA) with maximum 32 elements, while the receiving side (Rx) employs a dual-polarized ($\pm 45°$) onmi-directional array (ODA) with maximum 56 elements. The radiation pattern coverage of these two kinds of antennas are shown in Table I, angular ranges in which can involve most of the paths on both ends.What's more, all antennas had been calibrated in an anechoic chamber. During our measurement, the transmission power is 26 dBm, the channel sampling rate is 54.389, and the length of the periodic pseudo-random binary sequence is 63.

TABLE I
ANTENNA PARAMETERS

Antenna	Azimuth coverage	Elevation coverage
ODA	$-180° \sim 180°$	$-55° \sim 90°$
UPA	$-70° \sim 70°$	$-70° \sim 70°$

B. Measurement Scenario

Extensive measurement was conducted in a 18-floor building. Layout of the second floor is illustrated in Fig. 2. During the measurement, Tx was located on the top of a lower building with its height set to be zero and the arrow shows the reference direction. The Rx was fixed with antenna height of about 1.8m on a trolly and the short arrow indicates the measurement spot while the long arrow indicates the measurement route. Direction of the arrow is the moving direction, reference direction of the long route may be the same or the opposite. The walls along the corridor and between the rooms are made of bricks with plasterboard on the surface. The floor is covered with marbles. The doors of the rooms are wooden. We measured the first 9 floors in this building, and each floor has the similar layout except for the first floor, so during our measurement, to facilitate the comparison, we just need to ensure the measurement spots or routes corresponding to the same position. The positions of one measurement spot and route are shown in Fig. 3. Height differences between Tx and Rx are as shown in Table II.

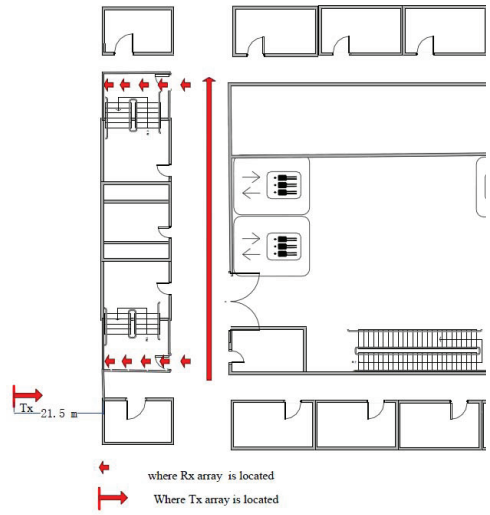

Fig. 2. Layout of the measurement scenario. Horizontal distance between Tx and Rx is 21.5m. All of the measured 9 floors have the similar layout. Reference direction of all the measurement spots are the same and the arrow of the long route indicates the moving direction, reference direction will either be the same or the opposite.

TABLE II
HEIGHT DIFFERENCE BETWEEN RX AND TX

Floor	1	2	3	4	5	6	7	8	9
Height difference(m)	-10	-4.8	0.8	2.6	6.4	9.8	13.8	17	21

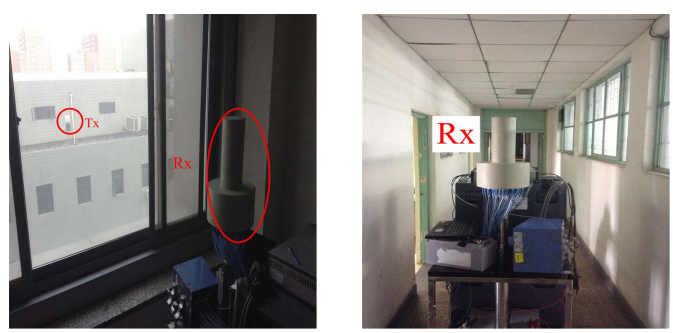

(a) Measured spot near the window (b) Measured route along a corridor

Fig. 3. Measurement spot or route

III. DATA PROCESSING

During data processing, the channel impulse responses are calculated from the raw data firstly, then the space-alternating generalized expectation maximization (SAGE) algorithm is utilized to get the channel parameters. Every 4 snapshots are fed to SAGE to generate one set of channel parameters. Each sage result contains a maximum resolved path number of 100 in the form of $\{\tau_l, \varphi_{AoA,l}, \phi_{AoA,l}, \varphi_{AoD,l}, \phi_{AoD,l}, \alpha_l, f_l\}$, which refer to delay, AoA, EoA, AoD, EoD, polarization matrix, and Doppler shift of the lth path, respectively.

A. Angular Spread

The cluster AS, which is the second moment of the propagation angles, can be calculated by equation (1)

$$\sigma_{AS,k} = \sqrt{\sum_{l=1}^{L_k} (\varphi_{l,k} - \mu_k)^2 \cdot P_{l,k} \Big/ \sum_{l=1}^{L_k} P_{l,k}} \tag{1}$$

where $P_{l,k}$ represents the power, and $\varphi_{l,k}$ refers to the angle value of the lth path of the kth cluster, including AoA, AoD, EoA, EoD. For a cluster, L_k denotes the total path number in it. μ_k is the mean angle value of the kth cluster, which is given by

$$\mu_k = \sqrt{\left(\sum_{l=1}^{L_k} \varphi_{l,k} \cdot P_{l,k}\right) \Big/ \left(\sum_{l=1}^{L_k} P_{l,k}\right)}. \tag{2}$$

In order to avoid the angular ambiguity caused by the origin of the coordinate system, we adopt the method proposed in [14].

B. Delay Spread

The root mean square (rms) delay spread (DS) is calculated to be the standard deviation of the excess delay weighed with the power, i.e.

$$\tau_{rms,k} = \sqrt{\sum_{l=1}^{L_k} \tau^2{}_{l,k} P_{l,k} \Big/ \sum_{l=1}^{L_k} P_{l,k} - \left(\sum_{l=1}^{L_k} \tau_{l,k} P_{l,k} \Big/ \sum_{l=1}^{L_k} P_{l,k}\right)^2} \tag{3}$$

where $\tau_{l,k}$ denote the excess delay of the lth path of the kth cluster.

IV. Analysis of Measurement Data

A. Comparison of Clustering in 2D and 3D

Algorithm introduced in [12] is adopted to identify clusters in both 2D and 3D in O2I scenario. As we can at most plot three dimensions, only delay, AoA, AoD can be seen from the figures. For one measurement spot, estimated MPCs extracted from SAGE results are presented in Fig. 4, the size of the ball is proportional to the power of the path and MPCs with the same color are within the same cluster. Fig. 4 (b) is the clustering results in 3D while Fig. 4 (a) is in 2D. Note that MPCs of a cluster in 2D are divided into several clusters in AoA-AoD-EoA-EoD-delay domains (see MPCs in the red circle in Fig. 4). In order to compare the clustering performance in 2D and 3D, we analyze the specific MPCs, i.e. MPCs in red circle in Fig. 4, and clustering results in 3D are demonstrated in Fig. 5. MPCs of different clusters in Fig. 5 (a) seem to have not been separated in AoD-AoD-delay domains. Considering the elevation domain and give the clustering results in EoA-EoD-delay domains, MPCs of different clusters are obviously separated. As Fig. 5 shows, MPCs within one cluster in 2D are divided into three clusters and each cluster contains MPCs with similar parameters, leading to smaller cluster MCD values. Since many MIMO channel models are based on cluster characteristics, smaller cluster MCD values offer the opportunity to more accurately model the 3D MIMO channels.

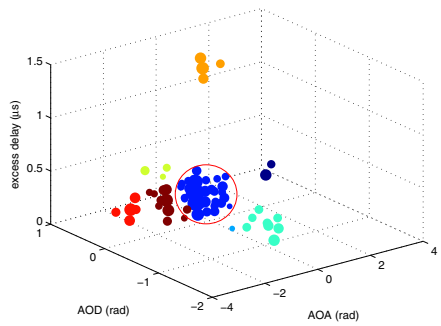

(a)

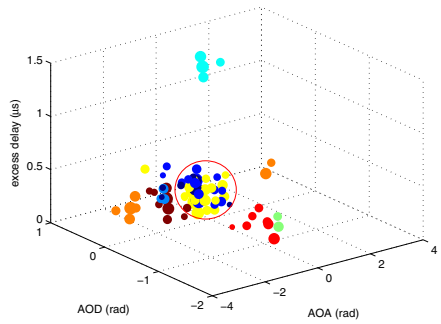

(b)

Fig. 4. Clustering results of a snapshot both in 2D and 3D. In (a), MPCs in a wide angular range belong to a same cluster while in (b), they are divided into several clusters.

B. Impact of Height Difference on Clustering

Since height difference exists in our measurement, angular characteristics may be different when Rx located on different floors. Using equation (1)-(3), cluster parameters in different floors are obtained and presented in Table III. Cluster number, cluster azimuth AS of arrival and departure, cluster elevation AS of arrival and departure are represented by CluNum, CASA, CASD, CESA, CESD respectively.

As can be seen from Table III, when the height difference is small, for example, the 2nd and 3rd floor (see in Table II), we have fewer clusters and smaller cluster AS. This is supposed to be the results of a large number of paths between Rx and Tx experiencing very little dispersion on both ends (almost the same with general 2D O2I channel models), thus a less number of clusters and smaller AS are obtained. As the height difference increases, more and more paths will experience more scattering and reflection, then generate more clusters and greater AS. By analyzing the relationship between height difference and CluNum, Fig. 6 is obtained. As it shows, CluNum increases with the increase of the height difference between the two ends, consistent with the left-part Gaussian distribution. The maximum CluNum is 16.62 with the height difference 16.5. However, as we know, when

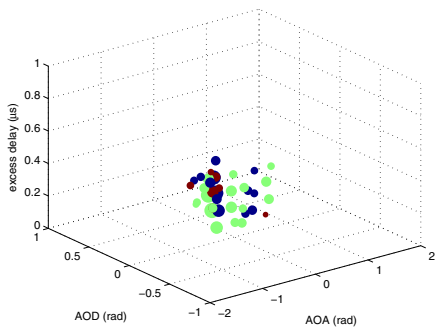

(a)

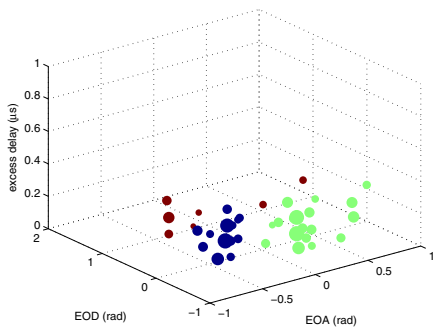

(b)

Fig. 5. Clustering results of the extracted MPCs in 3D. MPCs in AoA-AoD-delay domains seem not to be separated show good clustering effects in EoA-EoD-delay domains.

TABLE III
HEIGHT DIFFERENCE BETWEEN RX AND TX

Floor	CluNum	CASA (°)	CASD (°)	CESA (°)	CESD (°)
1	15.2	8.5	6.1	10.6	5.1
2	12.5	11.3	5.9	7.7	4.7
3	13.4	10.6	5.9	5.1	4.8
4	14.0	10.9	6.1	4.8	5.3
5	15.4	11.5	6.4	8.7	5.7
6	16.8	11.9	5.9	9.5	5.6
7	17.4	12.3	6.7	9.8	6.3
8	15.6	11.9	7.1	7.8	7.6
9	16.5	13.6	6.8	6.8	7.0
Mean	14.3	11.2	6.2	6.8	5.5

the height difference is too big, the transmitting signal will experience more scattering or reflection, resulting in fewer MPCs arriving at the Rx, and also less CluNum, as latter part of Fig. 6 shows. Since the number of the floors we measured here is small, statistical characteristics are not persuasive, further studies will be possible to see whether the cluster parameters can be modeled by the height difference in 3D O2I scenario. Here, we also give the mean values of the cluster

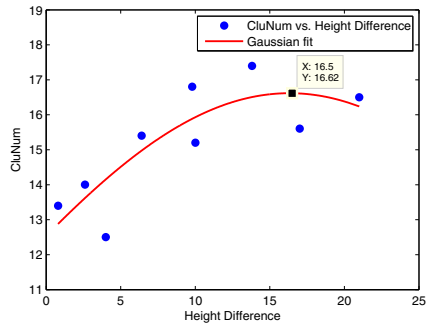

Fig. 6. Gaussian distribution of the height difference and CluNum

parameters in Table III.

C. Distribution of Cluster Parameters

For intra-cluster parameters, statistical results of AS are shown in Fig. 7. Lognormal fit can well fit the CASA, CASD, CESA, CESD, and mean values of these spreads are 11.9 °, 6.2 °, 7.1 °, 5.5 ° respectively. Fig. 8 shows the cluster DS, which is modeled by Lognormal distribution with the mean value of 7.1 ns.

For inter-cluster parameters, the probability density function of the cluster number is shown in Fig. 9. Most of our measurement spots have more than 12 clusters, and the mean value is 14.4. Fig. 10 presents the distribution of the path number in clusters. Mean value of the Lognormal distribution is 4.9 per cluster.

V. CONCLUSION

In this paper, we have performed a comparison of clustering performance between 2D and 3D and analysis of cluster parameters with different height differences between Tx and Rx. Based on the wideband MIMO measurements of O2I scenario at 3.5 GHz, we have found that clustering in 3D can improve the clustering performance. Using the distance function MCD, MPCs within one cluster in 2D may be reclustered and result in more clusters and smaller cluster MCD, which means smaller differences between MPCs per cluster, and it is very useful for 3D MIMO channel modeling. Taking into account the height difference between Tx and Rx, cluster characteristics vary on different floors due to different scattering and reflection. The smaller the height difference, the smaller cluster parameters will be. We also draw a prospect for further studies to see whether the cluster parameters can be modeled by the height differences. Cluster parameters including intra-cluster parameters and inter-cluster parameters are also presented in this paper. Mean values are 7.1 ns, 11.9 °, 6.2 °, 7.1 °, 5.5 °, 14.4, 4.9 for DS, CASA, CASD, CESA, CESD, CluNum, mean path number per cluster respectively.

ACKNOWLEDGMENT

The research is supported by China Mobile Research Institute, National Key Technology Research and Development Program of the Ministry of Science and Technology of China

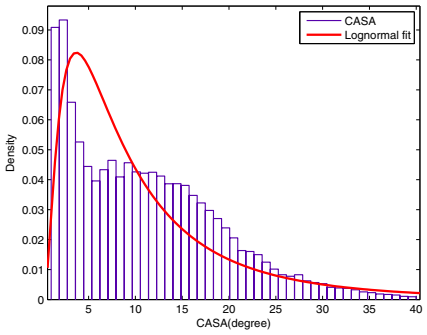

(a) CASA

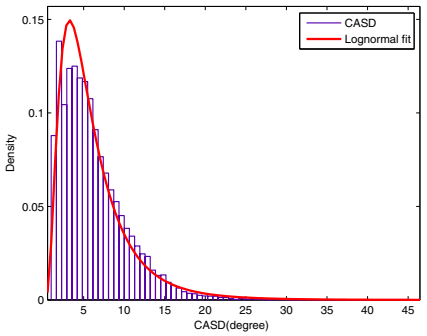

(b) CASD

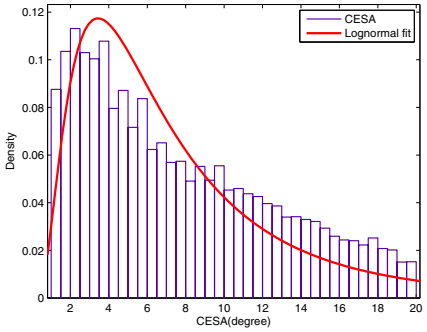

(c) CESA

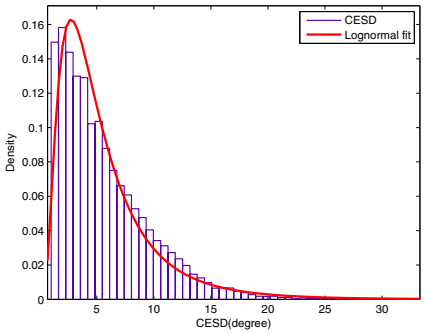

(d) CESD

Fig. 7. Lognormal distribution of angular spread within a cluster

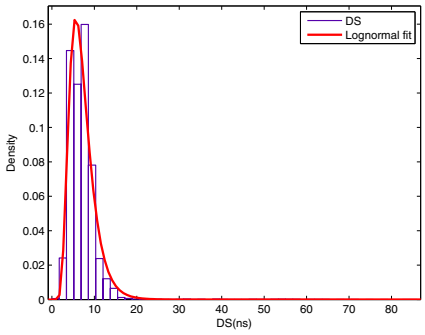

Fig. 8. Distribution of delay spread within a cluster

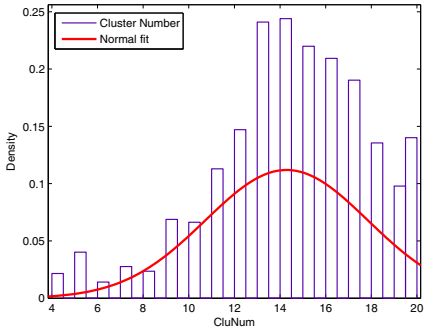

Fig. 9. Normal distribution of the cluster number

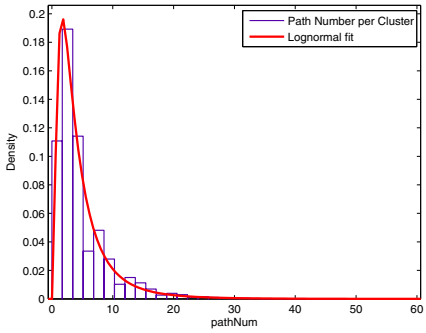

Fig. 10. Lognormal distribution of the path number in one cluster

and project name is ”Research and Development for Multi-Dimensional Broadband Time-Varying Channel Emulator” with NO. 2012BAF14B01, National Science and Technology Major Project of the Ministry of Science and Technology and project name is ”Research and Development of 3D MIMO Technique” with 2013ZX03003009, Program for New Century Excellent Talents in University of Ministry of Education of China, NCET-11-0598.

REFERENCES

[1] A. Molisch, ”Modeling the MIMO propagation channel,” *Beigian Journal of Electronics and Communications*, no. 4, pp. 5-14, 2003

[2] L. Correia, Ed., ”Mobile Broadband Multimedia Netwoks.” Published by *Acadamic Press*, 2006

[3] M. Kiessling, J. Speidel, I. Viering, and M. Reinhardt, "Statistical prefiltering for MMSE and ML receivers with correlated MIMO channels," in *Proc. IEEE Wireless Communications and Networking* (*WCNC 2003*), vol. 2, 2003, pp. 919-924.

[4] K. Li, M. Ingram, and A. Van Nguyen, "Impact of clustering in statistical indoor propagation models on link capacity," *IEEE Trans. Commun.*, vol. 50, no. 4, pp. 521-523. April 2002.

[5] C. Huang, J. Zhang, X. Nie and Y. Zhang, "Cluster Characteristics of Wideband MIMO Channel in Indoor Hotspot at 2.35 GHz," in *Vehicular Technology Conference Fall* (*VTC 2009-Fall*), *2009 IEEE 70th*, 20-23 Sept/ 2009.

[6] E. Bonek, N. Czink, V. M. Holappa, et al, " Indoor MIMO measurements at 2.55 and 5.25 GHz-a comparison of temporal and angular characteristics[J]," *Procc. of the IST Mobile Summit*, 2006.

[7] L. Hentila, Elektrobit, Oulu, M. Alatossava, N. Czink, P.Kyosti, "Cluster-level parameters at 5.25 GHz indoor-to-outdoor and outdoor-to-indoor MIMO radio channels," in *Mobile and Wireless Communications Summit*, *2007. 16th IST*, 1-5 July 2007.

[8] S. Wyne, N.Czink, J. Karedal, et al, "A cluster-based analysis of outdoor-to-indoor office MIMO measurements at 5.2 GHz," in *Vehicular Technology Conference, 2006. VTC-2006 Fall. 2006 IEEE 64th*. 25-28 Sept. 2006.

[9] 3GPP Technical Rep. 36.913, Home eNode B (HeNB) Radio Frequency(RF) requirements analysis (Release 8), Jun.,2008

[10] M. Shafi, et al., The impact of elevation angle on MIMO capacity, *IEEE ICC06*, Jun. 2006.

[11] Wireless World Initiative New Radio, WINNER+ final channel models, 2010.

[12] N. Czink, P. Cera, J. Salo, E. Bonek and Nuutinen, " A Framwork for Automatic clustering of Parametric MIMO Channel Data Including Path Powers," in *Proc. IEEE 64th VTC-2006 Fall*, 2006, pp. 1-5.

[13] N. Czink, P.Cera, J.Salo, E. Bonek, J.- P. Nuutinen, J. Ylitalo, "Improving clustering performance using multipath component distance," *Electronics Letters*, Volume 42, Issue 1, 5 January 2006, P. 33-35, July 2012.

[14] W. Dong, J. Zhang, X. Gao, P, Zhang and Y. Wu, "Cluster Identification and Properties of Outdoor Wideband MIMO Channel," in *Pro. IEEE 66th, VTC-2007 Fall*, 2007, pp. 829-833.